Applied Physics Letters

Back focal plane imaging spectroscopy of photonic crystals

Cite as: Appl. Phys. Lett. **101**, 081904 (2012); https://doi.org/10.1063/1.4746251
Submitted: 09 May 2012 . Accepted: 31 July 2012 . Published Online: 21 August 2012

Rebecca Wagner, Lars Heerklotz, Nikolai Kortenbruck, and Frank Cichos

Back focal plane imaging spectroscopy of photonic crystals

Rebecca Wagner, Lars Heerklotz, Nikolai Kortenbruck, and Frank Cichos[a)]
Molecular Nanophotonics, Institute of Experimental Physics I, Leipzig University, Linnéstrasse 5, 04103 Leipzig, Germany

(Received 9 May 2012; accepted 31 July 2012; published online 21 August 2012)

Back focal plane imaging spectroscopy is introduced to record angle resolved emission spectra of 3-dimensional colloidal photonic crystals. The auto-fluorescence of the colloids is used to quickly map the photonic band structure up to 72 % of the solid angle of a semisphere with the help of a high numerical aperture objective. Local excitation provides spatially resolved information on the photonic crystal's optical properties. The obtained fractional density of states allows direct conclusions on the crystal's stacking faults or defects. © *2012 American Institute of Physics*. [http://dx.doi.org/10.1063/1.4746251]

Photonic crystals (PCs) are materials with periodically varying refractive index. They possess a complex anisotropic optical dispersion relation, which is known as the photonic band structure and very similar to the electronic band structure of semiconductors. The optical properties of PCs are intrinsically linked to its structure.[1–3] Thus, defects, which are generated accidentally[3–5] during the production procedure or intentionally, for example to create waveguides,[6] cause local optical defect modes. Therefore efficient methods with spatial, spectral and angular resolution are required to study light propagation in PCs.

Common techniques are reflection or transmission spectroscopy, which can be carried out at variable angle of incidence to map the photonic band structure.[3–5,7,8] However, they illuminate rather large sample areas, therefore averaging over different crystal domains including their structural defects. Thus, stacking faults which often occur in colloidal PCs are for example hard to identify. Furthermore, the incident light needs to be coupled into the PC, which is not necessarily possible for all photonic modes due to symmetry reasons.[9,10] Therefore internal light sources such as fluorescent chromophores have been introduced to reveal similar information as compared to transmission experiments.[1,11] Fluorescence spectra for a few emission angles have been reported by different groups.[11–15] A detailed study was carried out by Brzezinski *et al.* measuring angle resolved fluorescence spectra from 76% of the solid angle of a semisphere for an inverted fluorescent opaline PC.[2] The recorded emission spectra revealed a threefold symmetry as expected for a well defined fcc crystal structure. However, these experiments have been very time-consuming as the position of the detector had to be changed for every measurement at a certain angle. A microscopic approach has been introduced by Barth *et al.*[1] Emitters in an fcc polystyrene PC were excited by a focused laser in a confocal microscopy setup. A circular aperture was used to select a fraction of the fluorescent light leaving the microscope objective that corresponded to certain emission directions. By scanning the aperture across the beam, emission spectra for different emission angles have been recorded.

Here we introduce back focal plane (BFP) imaging spectroscopy to allow for a fast spectral imaging of the photonic band structure. We demonstrate that emission spectra over a large angular range can be quickly recorded in a microscopy setup. These spectra provide information on the angular dependence of the fractional density of states (FDoS),[1] which characterizes the anisotropic light emission in the PC.

BFP imaging has been shown to provide information on the anisotropic light propagation in crystals[16] or the emission anisotropy of single fluorescent molecules.[17] It relies on the fact, that aplanatic microscope objectives fulfill the Abbe sine condition $r = nf\sin(\vartheta)$.[16,18] This condition states, that light, that has been emitted from the focal point (focal distance f) under an angle ϑ with the optical axis, leaves the microscope objective lens at a distance r parallel to it. Light emitted from any other arbitrary position, but under the same angle ϑ, will not be parallel to the optical axis behind the objective lens but still have the distance r in the BFP. Thus, all light that has been emitted in the same direction is focused into the same point of the BFP (Fig. 1(a)). Introducing the numerical aperture of the objective lens $\mathrm{NA} = n\sin(\vartheta_{\max}) = r_{\max}/f$, the refractive index n of the medium surrounding the emitter, and the maximum distance from the optical axis given by the size of the objective's exit pupil r_{max} leads to the following equation:

$$\sin(\vartheta) = \frac{r\mathrm{NA}}{r_{\max} n}. \tag{1}$$

This directly relates a BFP image point to a certain propagation direction incident to the microscope objective. The numerical aperture of the microscope objective determines the angular range that can be studied. Using isotropic emitters embedded in a material, therefore, provides the possibility to study the anisotropic light propagation in the material surrounding the emitter. Emitters with a wide emission bandwidth further allow to cover a large spectral range in the emission anisotropy study.

We have integrated a BFP imaging system in a home-built confocal microscope. A high NA oil objective (Olympus UPLSAPO 100XO, NA = 1.4) is used to focus the excitation light (488 nm line of an Argon ion laser) to a focus diameter of about 300 nm on the sample. The emitted light is

a)Electronic mail: cichos@physik.uni-leipzig.de.

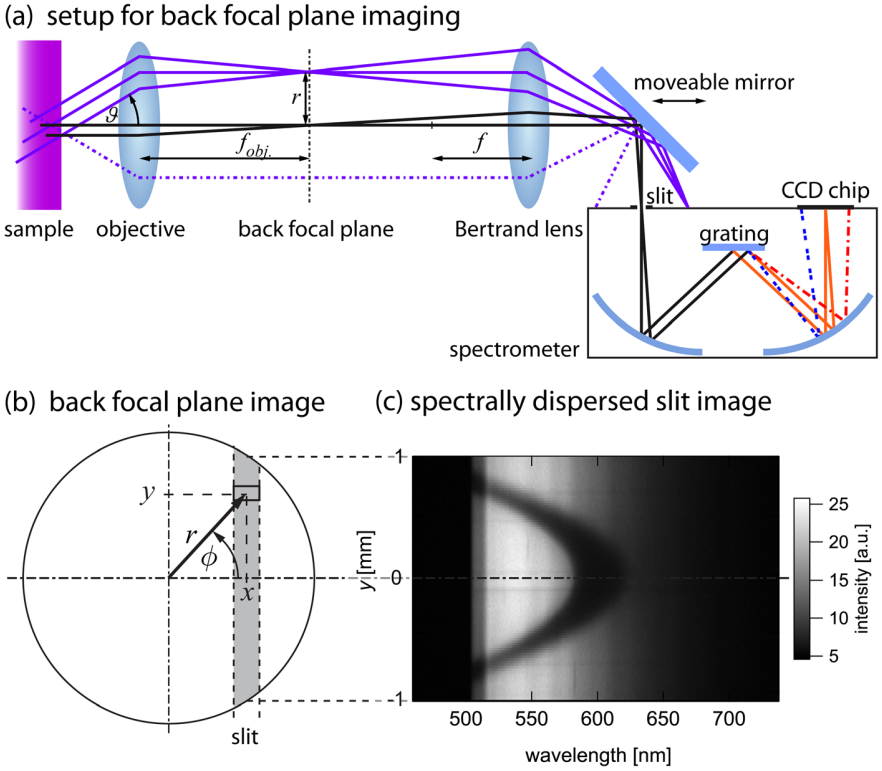

FIG. 1. Sketch of the BFP measurement principle: (a) The fluorescence from the sample is collected by a microscope objective lens. Light emitted in a certain direction ϑ is focused into a point in the objective's BFP with distance r from the optical axis. The BFP of the objective lens is imaged onto the spectrograph's entrance slit (perpendicular to drawing plane). The divergence of the beam imaged to the spectrograph's entrance slit is about 0.4°. Thus, light entering the spectrometer is assumed to be parallel. (b) The spectrograph slit at position x from the center selects a vertical line (shaded region) from the BFP image (circular area). An increasing radius r in the BFP image corresponds to different polar emission angles ϑ according to Eq. (1). The emission direction in the sample is further defined by the azimuthal angle ϕ. (c) Spectrally dispersed fluorescence intensity emitted by the photonic crystal sample along the direction of the entrance slit y for the slit position $x = 0$. Each vertical point y along the slit therefore corresponds to a spectrum for the emission under the angles (ϑ, ϕ). The stop band of the PC is visible as dark arc.

collected by the same objective lens and passed through a dichroic (DMLP505, Thorlabs) and a longpass filter (502ALP, omega optical) to remove residual excitation light. The remaining fluorescence light is focused by a tube lens onto an avalanche photodiode (MPD, Micro Photon Devices PDM series) to image the sample in confocal mode.

To record angle resolved fluorescence spectra in BFP imaging mode, the excitation focus is placed 4 μm deep in the sample and the detected fluorescence light is redirected to an imaging spectrometer (Acton SpectraPro-300i). More precisely, the BFP of the objective lens is imaged on the entrance slit of the spectrometer using a Bertrand lens, thereby reducing the beam diameter to 2.7 mm (Fig. 1(a)). The entrance slit of the spectrometer is closed to 80 μm and used to select a vertical line from the BFP image (shaded region in Fig. 1(b), the circle corresponds to the maximum size of the BFP image given by $r_{\max}$). This vertical line is spectrally dispersed and imaged on a liquid nitrogen cooled CCD with a 100 pixel × 1340 pixel chip (Princeton Instruments, LN/CCD). Each vertical line selected by the entrance slit thus results in 100 spectra of light emitted into different directions for each single measurement. An example of an image obtained in a single measurement on a colloidal photonic crystal sample is shown in Fig. 1(c). The image displays the unprocessed emission intensity along the slit position y at different wavelengths. To record emission spectra from all regions of the BFP, the BFP image is shifted across the entrance slit using a mirror as indicated in Fig. 1(a). With a BFP image of 2.7 mm in diameter, 35 measurements are carried out to cover the whole image with a slit width of 80 μm. Following this procedure, angular emission spectra can be recorded up to a maximum emission angle of $\vartheta_{\max} = 73.5°$.

To determine the angular resolution of the method, we refer to the angles ϑ (see Fig. 1(a)) and ϕ (see Fig. 1(b)), which define the emission direction. If we consider an emission at a polar angle ϑ and an azimuthal angle $\phi = 0°$, the resolution $\Delta\vartheta$ is limited by the entrance slit width. The resolution in the azimuthal angle $\Delta\phi$ is limited by the pixel size, since each line of the CCD is recording an independent spectrum. If the emission direction under an angle ϑ changes to $\phi = 90°$, the pixel size is now determining $\Delta\vartheta$ and the slit width is limiting $\Delta\phi$. The angular resolution can therefore be altered by changing the width of the entrance slit or the image size on the CCD. Further, both angular resolutions vary depending on the azimuthal angle for $\vartheta > 0°$ (see supplement Fig. S1). For a slit width of 80 μm and a pixel size of 20 μm, a lower resolution limit of 1.6° and an upper limit of about 8.8° for $\Delta\vartheta$ has been calculated. For $\Delta\phi$, the resolution is best for large ϑ $(\Delta\phi = 1.6°)$ but there is no resolution at the center of the BFP image. For details on the calculation, see the supplementary material.[19]

The gain in angular resolution of BFP imaging is actually at the cost of spatial resolution since the depth of focus gets infinitely large. Especially in the case of an extended fluorescent structure, the light is collected from all regions illuminated by the excitation light. Therefore there is no spatial resolution along the optical axis. The lateral resolution is, however, retained due to the localized excitation focus. Using a localized excitation focus in combination with a local emitter like a single fluorescent bead or single molecule would nevertheless reintroduce spatial resolution along the optical axis to the method.

To demonstrate the application of BFP imaging spectroscopy for the measurement of photonic band structures, we have studied colloidal PCs prepared by vertical deposition of 260 nm polystyrene (PS) spheres (Duke Scientific).[19] The spheres form a three dimensional fcc-lattice with the (111)-plane parallel to the substrate surface.[20–22]

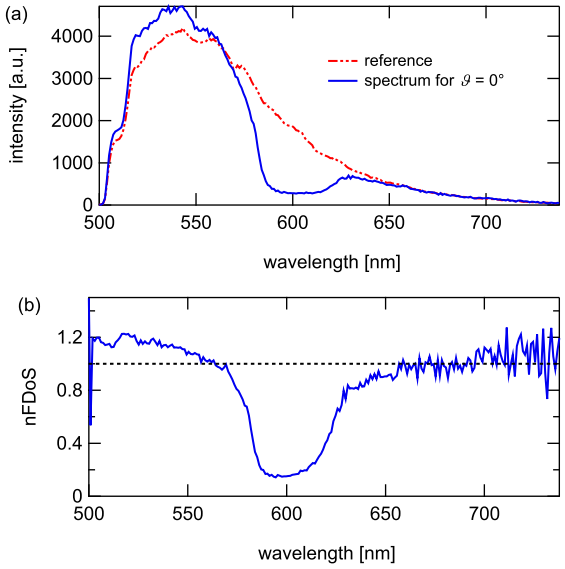

FIG. 2. (a) Fluorescence spectrum for emission under $\vartheta = 0°$ normalized to the long wavelength tail of a reference spectrum. The emission spectrum clearly shows a reduced emission intensity as compared to the reference in the stop band region. (b) Ratio of the emission and the reference spectrum as a function of wavelength. The ratio corresponds to the normalized fractional density of states (nFDoS), which has a minimum at the position of the stop band and reveals a slight enhancement at the low wavelength side.

As the PS beads are weakly auto-fluorescent in the spectral range from 500 nm to 750 nm,[23,24] they can be used for BFP imaging without any additional doping by fluorescent dyes. Fig. 1(c) shows an example of a single unprocessed measurement on a colloidal PC where the slit has been positioned in the center of the BFP ($x = 0$). Every row on the CCD chip delivers the emitted intensity over the wavelength for a vertical position y within the slit. Since emission in the direction of the stop band is inhibited, the photonic stop band is directly visible as a dark arc. The emission angles ϑ corresponding to every CCD row can be calculated using Eq. (1).

As the intensity detected at different angular directions varies with the detection angle, the spectra recorded in a measurement are normalized to the long wavelength tail of a reference spectrum between 660 nm and 720 nm. This spectral region corresponds to frequencies well below the photonic stop band where the PC resembles an effective homogeneous medium. To record a reference spectrum, we choose an emission direction where no effect of the photonic band structure is expected (here $\vartheta = 38°$, $\phi = 317°$). A comparison of the reference and an actual emission spectrum for an angle of $\vartheta = 0°$ ($x = 0$, $y = 0$) of the PC is depicted in Fig. 2(a). Calculating the ratio of the emission and reference spectrum (Fig. 2(b)) delivers the normalized fractional density of states (nFDoS) in a certain emission direction,[1] correcting at the same time for the transmission through dichroic and longpass filter. The nFDoS then indicates a modification of light propagation as compared to a homogeneous medium. The determined nFDoS (Fig. 2(b)) reveals a characteristic dip at about 600 nm, which nicely corresponds to the Bragg reflection of the (111) lattice planes as expected for normal incidence and a bead size of 258 nm. The nFDoS minimum in the stop band is however non-zero (≈ 0.15) due to structural defects and the emission from interfacial regions of the PC, where the stop band is not fully developed. Further, the nFDoS suggests a slightly enhanced emission at the short wavelength edge of the stop band, which has been observed in other studies before.[1]

The spectral shift of the stop band with the emission angle can be obtained by analyzing the emission spectra at different angles ϑ. The result is depicted in Fig. 3(a), where the nFDoS value is plotted color-coded against emission angle and wavelength. Starting at 600 nm for an emission angle of $\vartheta = 0°$, the stop band shifts to lower wavelength for increasing emission angle as expected for Bragg reflections

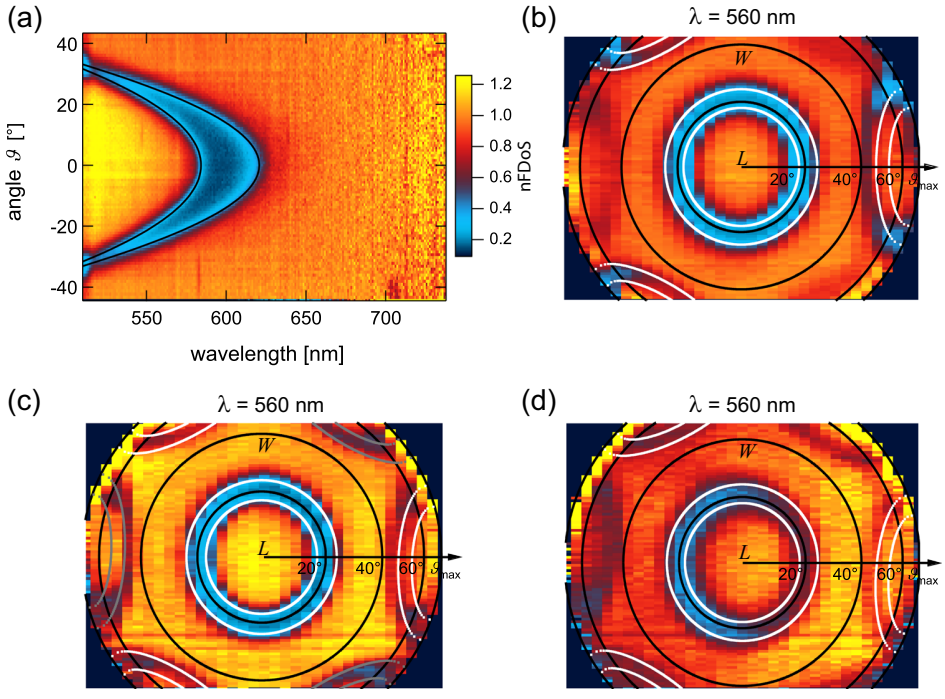

FIG. 3. (a) Measured nFDoS for a slit position $x = 0$ plotted color-coded against emission angle and wavelength. The nFDoS has a minimum at the stop band position. The angle dependence of the stop band follows the prediction of band structure simulations (black lines). (b) For a certain wavelength, the polar plot of the nFDoS reflects the threefold symmetry of the fcc PC. The white lines indicate the simulated positions of the stop bands. The circular stop band appearing at small emission angles corresponds to the (111) lattice planes parallel to the sample substrate. At larger angles stop bands from the $(\bar{1}11)$, $(1\bar{1}1)$ and $(11\bar{1})$ lattice planes can be seen. The *L*-*W*-direction, in which the PC is grown, is indicated. Each stripe corresponds to one measurement with a certain position of the moveable mirror. (c) Stacking faults lead to sixfold symmetric patterns. (d) A nearby crack (3.3 μm to the right) reduces the depth of the stop band. The color scale is the same for all images.

on the (111) lattice planes of the fcc crystal. The experimental results are compared to numerical calculations for a polystyrene colloidal photonic crystal using the MIT photonic-bands (MPB) software package[25] (black lines in Fig. 3(a)). Both, experiment and simulation are found to be in perfect agreement.

Recording emission spectra of the PC for all other directions by shifting the BFP across the slit delivers the complete spectral information of the nFDoS within the range of accessible emission angles ($\vartheta = 0°…73°$ with the [111]-direction). From this data, a polar plot of the nFDoS at each wavelength may be constructed as depicted in Fig. 3(b). Since the (111) lattice planes are parallel to the sample substrate, the associated stop band emerges for the same emission angle ϑ for all angles ϕ at a fixed wavelength. It appears therefore as a circular region with minimal nFDoS values. Stop bands of other lattice planes are visible at larger emission angles ($\vartheta > 40°$) and result from the $(\bar{1}11)$, $(1\bar{1}1)$, and $(11\bar{1})$ lattice planes, which are not parallel to the sample surface. The white lines in Fig. 3(b) indicate the positions of the corresponding stop bands as obtained from the band structure calculations. The observed angular emission intensity at a certain wavelength and large emission angles ϑ thus obeys a threefold symmetry as expected for a fcc crystal structure. The orientation of these stop bands in the BFP image allows to conclude on the growth direction of the PC, which is the *L*-*W*-direction as confirmed by previous findings.[4,26,27]

In some cases an additional set of stop bands, rotated by 60° is observed. This results in a sixfold symmetry of the BFP image and is due to stacking faults such as a change from *ABC* to *CBA* stacking (twin structure) (Fig. 3(c)). Since the two structures differ by the positions of stop bands at larger angles the amount of *ABC* or *CBA* structure in the observed PC domain might be judged by the depth of the individual stop bands. This provides possibilities for the study of local structural defects in PCs. Accordingly, other defects such as different growth directions and their correlation to the appearance of cracks in the crystal structure can be studied. In the case of cracks, deformations of the position and depth of the stop band are observed. Fig. 3(d) displays the polar plot of the nFDoS recorded at a position 3.3 μm left of a crack. The (111) stop band is clearly less pronounced in direction of the defect (right edge of the image) and disappears directly at the crack due to the missing fluorescent structure. Correlating the depth of the stop band and the symmetry of the nFDoS with the position in the PC could therefore deliver a wealth of information on defect related distortions of the photonic crystal band structure.

In summary, we have applied back focal plane imaging to obtain angle resolved emission spectra from colloidal photonic crystals up to emission angles of 73° without moving or tilting the sample. The found photonic stop band positions correspond well to the theory predictions. The lattice structure and orientation can be deduced from the angular symmetry of the stop band position. In nearly all cases, a threefold symmetry of the PC is found as expected from the fcc structure. The influence of nearby defects on the stop bands can be revealed, which makes back focal plane imaging especially useful for the study and characterization of defects in photonic crystals. In combination with localized emitters, spatial resolution along the optical axis can be introduced to the method. Further, replacing the spectrograph by a suitable band pass filter provides even a direct imaging tool for photonic band structures at a fixed wavelength, which enables quick defect and structure characterization or a fast detection of growth direction in 3-dimensional PCs.[28]

We thank Georg Kropat for help with the data analysis program. R.W. thanks the Deutsche Forschungsgemeinschaft for financial support (project no. CI 33/5-2).

[1]M. Barth, A. Gruber, and F. Cichos, Phys. Rev. B. **72**, 085129 (2005).
[2]A. Brzezinski, J.-T. Lee, J. D. Slinker, G. G. Malliaras, P. V. Braun, and P. Wiltzius, Phys. Rev. B **77**, 233106 (2008).
[3]A. V. Baryshev, A. B. Khanikaev, R. Fujikawa, H. Uchida, and M. Inoue, J. Mater. Sci.: Mater. Electron. **20**, 416 (2009).
[4]J. F. Galisteo-López, E. Palacios-Lidón, E. Castillo-Martínez, and C. López, Phys. Rev. B **68**, 115109 (2003).
[5]A. V. Baryshev, A. B. Khanikaev, R. Fujikawa, H. Uchida, and M. Inoue, Phys. Rev. B **76**, 014305 (2007).
[6]S. Kedia and R. Vijaya, Bull. Mater. Sci. **34**, 383 (2011).
[7]T. Maka, D. Chigrin, S. Romanov, and C. S. Torres, Prog. Electromagn. Res. **41**, 307 (2003).
[8]H. Miguez, V. Kitaev, and G. A. Ozin, Appl. Phys. Lett. **84**, 1239 (2004).
[9]W. M. Robertson, G. Arjavalingam, R. D. Meade, K. D. Brommer, A. M. Rappe, and J. D. Joannopoulos, Phys. Rev. Lett. **68**, 2023 (1992).
[10]F. López-Tejeira, T. Ochiai, K. Sakoda, and J. Sánchez-Dehesa, Phys. Rev. B **65**, 195110 (2002).
[11]M. Li, P. Zhang, J. Li, J. Zhou, A. Sinitskii, V. Abramova, S. Klimonsky, and Y. Tretyakov, Appl. Phys. B **89**, 251 (2007).
[12]S. G. Romanov, A. V. Fokin, and R. M. D. L. Rue, Appl. Phys. Lett. **76**, 1656 (2000).
[13]Y. Lin, J. Zhang, E. H. Sargent, and E. Kumacheva, Appl. Phys. Lett. **81**, 3134 (2002).
[14]L. Bechger, P. Lodahl, and W. Vos, J. Phys. Chem. B **109**, 9980 (2005).
[15]K. Baert, B. Kolaric, W. Libaers, R. A. L. Valle, M. D. Vece, P. Lievens, and K. Clays, Res. Lett. Nanotechnol. **2008**, 974072 (2008).
[16]M. Born and E. Wolf, *Principles of Optics: Electromagnetic Theory of Propagation, Interference and Diffraction of Light*, 7th ed. (Cambridge University Press, Cambridge New York, 2011).
[17]M. A. Lieb, J. M. Zavislan, and L. Novotny, J. Opt. Soc. Am. B **21**, 1210 (2004).
[18]L. Dai, I. Gregor, I. von der Hocht, T. Ruckstuhl, and J. Enderlein, Opt. Express **13**, 9409 (2005).
[19]See supplementary material at http://dx.doi.org/10.1063/1.4746251 for details on the angular resolution and on sample preparation.
[20]S. H. Im, M. H. Kim, and O. O. Park, Chem. Matter **15**, 1797 (2003).
[21]H. Cong and W. Cao, Langmuir **19**, 8177 (2003).
[22]S.-L. Kuai, X.-F. Hu, A. Hach, and V.-V. Truong, J. Cryst. Growth **267**, 317 (2004).
[23]K. D. Crawford and K. D. Hughes, J. Phys. Chem. B **101**, 864 (1997).
[24]K. D. Crawford and K. D. Hughes, J. Phys. Chem. B **102**, 2325 (1998).
[25]S. G. Johnson and J. D. Joannopoulos, Opt. Express **8**, 173 (2001).
[26]K. Wostyn, Y. Zhao, B. Yee, K. Clays, A. Persoons, G. de Schaetzen, and L. Hellemans, J. Chem. Phys. **118**, 10752 (2003).
[27]J. F. Galisteo, F. Garcia-Santamaria, D. Golmayo, B. H. Juarez, C. Lopez, and E. Palacios, J. Opt. A: Pure Appl. Opt. **7**, S244 (2005).
[28]"Fast measurement of photonic stop bands by back focal plane imaging" (unpublished).